Molecular Dynamics Simulation of Annular Flow Boiling in a Microchannel with 70000 Atoms

D.Toghraie, A.R.Azimian

Abstract—Molecular dynamics simulation of annular flow boiling in a nanochannel with *70000* particles is numerically investigated. In this research, an annular flow model is developed to predict the superheated flow boiling heat transfer characteristics in a nanochannel. To characterize the forced annular boiling flow in a nanochannel, an external driving force $\vec{F}_{ext}$ ranging from 1to12PN (PN= Pico Newton) is applied along the flow direction to inlet fluid particles during the simulation. Based on an annular flow model analysis, it is found that saturation condition and superheat degree have great influences on the liquid-vapor interface. Also, the results show that due to the relatively strong influence of surface tension in small channel, the interface between the liquid film and vapor core is fairly smooth, and the mean velocity along the stream-wise direction does not change anymore.

Keywords—Lennard-Jones Potential, Molecular Dynamics Simulation, Periodic Boundary Conditions (PBC), Non-Equilibrium Molecular Dynamics (NEMD), Annular Flow Boiling

I. INTRODUCTION

BOILING flow and phase change of a fluid are intriguing and challenging topics in the field of macroscale and nanoscale heat and mass transfer researches. A better understanding of these phenomena can enhance energy efficiency in engineering processes. In recent years, studies on modeling of flow boiling heat transfer in micro and nanochannels have become very active in academic societies. Empirical correlations are a convenient means for determining the flow boiling heat transfer characteristics in micro and nanochannels. But great progresses in computer science and computational techniques provide a possible resolution. It is possible to investigate microscopic boiling flow heat transfer characteristics by computer simulations. Molecular dynamics simulation is a powerful numerical method for gaining in-depth knowledge of such phenomenon at the atomic level. This method is an accurate but computationally expensive method. The main idea behind the classical molecular dynamics is calculation of Newton's equation of motion for each particle in order to extract thermodynamical properties such as pressure and transport properties.

During past years, molecular dynamics simulation has emerged as a powerful tool for probing the microscopic behavior of fluids at interfaces [1]. Also, this method is a very promising method to investigate heat and mass transfer in micro and nano scale, especially for liquids and dense gases, whether the corresponding continuum equations are valid or not [2]. Long et al [3] studied the evaporation of liquid Argon droplets exposed to both subcritical and supercritical surrounding using 5600 particles, 27000 particles and 100000 particles. Their results for evaporation rate obtained by molecular dynamics simulation agree with the existing theoretical and experimental results.Lukes et al. [4] predicted the thermal conductivity of solid thin films in the direction perpendicular to the film plane using the molecular dynamics simulation. They found some temperature and computational size limitations on the applicability of molecular dynamics to the study of solid systems.The molecular dynamics simulations of the vaporization phenomenon of an ultra-thin layer of liquid Argon on a Platinum surface were performed by Yi et al. [5]. Their results were in good agreement with existing knowledge of vaporization of a similar macroscopic system. They also concluded that after complete evaporation and upon reduction of the wall temperature, condensation takes place leading to the reconstruction of the initial liquid layer. Wong et al. [6] investigated the evaporation process by performing a non-equilibrium molecular dynamics simulation. They obtained transient density, temperature and pressure profiles by statistical methods. They reached reasonable agreements between the evaporation coefficients from their NEMD simulations and those from the modified transition state theory.Dong et al. [7] performed molecular dynamics simulation of R141b boiling flow in nanochannel. They obtained temperature distribution, density and surface tension profiles in a cuboid cell in which a temperature gradient was set at both ends. They concluded that the characteristics of the liquid-vapor interface heavily depend on the saturated temperature and the degree of superheat.Ji and Yan [8] studied the liquid–vapor–solid system near triple–point of flow boiling in a microchannel heat sink by molecular dynamics simulation. They concluded that the number of fluid molecules, the solid wall temperature and the simulation size are some key parameters which will be helpful for the development of a microchannel phase change heat sink. We have carried out NEMD simulations of annular boiling flow of simple Lennard–Jones fluids subject to an inlet driving force in a nanochannel. The objective of this paper is to examine the effect of modified Lennard-Jones potential function on the

D. Toghraie is with the Isfahan University of Technology, Isfahan, Iran (Corresponding author to provide phone: 0098-913-322-1167; fax: 0098-311-2238384; E-mail: davoodtoghraie@ gmail.com).
A.R.Azimian is with the Isfahan University of Technology, Isfahan, Iran (E-mail: azimian@cc.iut.ac.ir).

World Academy of Science, Engineering and Technology
International Journal of Physical and Mathematical Sciences
Vol:5, No:6, 2011

heat flux, velocity, temperature and surface tension profiles in order to understand the boiling flow behavior in nanochannel geometry better.

II. SIMULATION PROCEDURE

In this paper, molecular dynamics simulations are carried out to characterize the forced annular boiling flow in a nanochcannel. Argon molecules moving in a nanochannel bounded by two solid walls on the x-axis are subjected to a streaming driving force at the inlet. The initial configuration is shown in Fig.1. In this figure, the Argon molecules were divided into three regions: the vapor molecules are moving along the center of the channel and the liquid molecules comprise two thin annular films along the channel walls sandwich the vapor phase portion. The size of the simulation domain is $45 \times 45 \times 120\sigma^3$. A total number of *70000* Argon atoms are placed and simulated in this domain. Each atom is spaced 1.15σ from its neighboring atoms in all three directions. At the bottom and top surfaces, wall boundary conditions are applied. Also, the system has doubly periodic boundary conditions in the x and y directions. The velocity of an atom crossing the x and y boundaries remains unchanged. Each solid wall consists of three layers of Platinum molecules. Also, periodic boundary conditions with respect to the number of molecules are applied along the x- and y-directions.
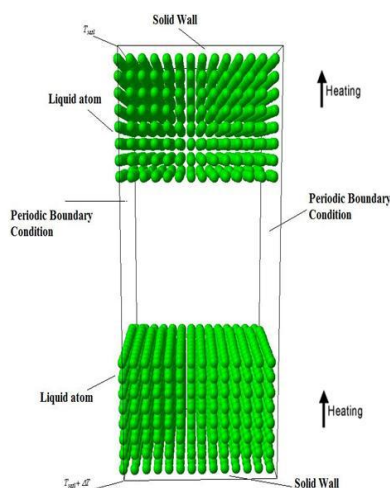

Fig. 1 Simulation system configuration of a nanochannel

Before performing MD simulation, an integration method for the equation of motion, the potential model and the simulation cell was determined. All the fluid molecules are supposed to abide by Newton's second law in MD simulations. For translational motion of a spherically symmetric molecule, when a two-body potential is determined, the force acting on the molecule can be expressed as the gradient of the potential function; in other words,

$$\vec{F}_i = \sum_{i \neq j} F_{ij} = m_i \frac{d^2 \vec{r}_i}{dt^2} = m_i \frac{d\vec{v}_i}{dt} \tag{1}$$

$$\vec{F}_{ij} = -\vec{\nabla}(\phi + \phi_w)$$

The MD simulations were carried out with Lennard-Jones particles that interact to each other via modified Lennard-

Jones potential function in the NVT ensemble. The interactions between simple liquid particles are modeled using the modified Lennard-Jones potential as defined by Stoddard and Ford (1973) [9]:

$$\phi(r_{ij}) = \left\{ 4\varepsilon \left[\left(\frac{\sigma}{r_{ij}} \right)^{12} - \left(\frac{\sigma}{r_{ij}} \right)^6 \right] \right\} \tag{2}$$
$$+ \left\{ 4\varepsilon \left[6 \left(\frac{\sigma}{r_c} \right)^{12} - 3 \left(\frac{\sigma}{r_c} \right)^6 \right] \right\} \left(\frac{r_{ij}}{r_c} \right)^2 - \left\{ 4\varepsilon \left[7 \left(\frac{\sigma}{r_c} \right)^{12} - 4 \left(\frac{\sigma}{r_c} \right)^6 \right] \right\}$$

Where $r_{ij} = |r_i - r_j|$ is the distance between the centers of spherical particles i and j, ε is the maximum potential depth and it is a parameter corresponding to the energy, σ is the length scale parameter and r_c is the cut-off radius. In this work, the cut-off radius for Lennard-Jones potential was set $r_c = 4.5\sigma$. In our previous work [10] results obtained for $3\sigma \leq r_c \leq 4.5\sigma$ were approximately the same within small fluctuations. However, decreasing r_c to less than 2σ produced significant changes in the potential, boundary conditions and other results [11]. Hence, for the purpose of physical understanding, in the present study, Argon is used as the LJ fluid with the following potential parameters: $m = 6.63 \times 10^{-26} kg$, $\sigma = 3.045 A°$ and $\varepsilon = 1.67 \times 10^{-21} J$. The solid walls are represented by three layers of face centered cubic surface of Platinum molecules with parameters such as: $m_s = 3.24 \times 10^{-26} kg$, $\sigma_s = 2.475 A°$ and $\varepsilon_s = 0.835 \times 10^{-21} J$ [12],[13].

To study the wall effects on the velocity, surface tension and temperature profiles, two solid walls were placed, one at the bottom boundary and the other at the top boundary. The bottom wall temperature was held at a superheated temperature, i.e.: $T_{sat} + \Delta T$, where ΔT shows the degree of superheat, while the upper wall temperature was held at a saturation temperature T_{sat}. This superheat degree, which is the driving force for heat flux, allows us to create a constant temperature gradient between the bottom and top wall in the z direction. For solid-liquid interactions, the following modified Lennard-Jones potential function is used [13]:

$$\phi_w(r_{ij}) = \left\{ 4\varepsilon_{sf} \left[\left(\frac{\sigma_{sf}}{z} \right)^{12} - \left(\frac{\sigma_{sf}}{z} \right)^6 \right] \right\} \tag{3}$$
$$+ \left\{ 4\varepsilon_{sf} \left[6 \left(\frac{\sigma_{sf}}{r_c} \right)^{12} - 3 \left(\frac{\sigma_{sf}}{r_c} \right)^6 \right] \right\} \left(\frac{z}{r_c} \right)^2 - \left\{ 4\varepsilon_{sf} \left[7 \left(\frac{\sigma_{sf}}{r_c} \right)^{12} - 4 \left(\frac{\sigma_{sf}}{r_c} \right)^6 \right] \right\}$$

$$\sigma_{sf} = \left[\frac{1}{2^{13}} \frac{\varepsilon\sigma^{12}}{\sqrt{\varepsilon\sigma^6 \varepsilon_s \sigma_s^6}} \left(1 + \left(\frac{\varepsilon_s \sigma_s^{12}}{\varepsilon\sigma^{12}} \right)^{\frac{1}{13}} \right)^{13} \right]^{\frac{1}{6}} \tag{4}$$

$$\varepsilon_{sf} = \frac{\sqrt{\varepsilon\sigma^6 \varepsilon_s \sigma_s^6}}{\sigma_{sf}^6} \tag{5}$$

Where, the Kong mixing rule [14] is applied to the system for calculating σ_{sf} and ε_{sf}. The velocity Verlet method [15] was used for the integration of the Newtonian equation. In this

World Academy of Science, Engineering and Technology
International Journal of Physical and Mathematical Sciences
Vol:5, No:6, 2011

algorithm the following equations are used to calculate the particle's trajectories:

$$r(t + \delta t) = r(t) + v(t)\delta t + \frac{F(t)}{m}\frac{\delta t^2}{2} \qquad (6)$$

$$v(t + \delta t) = v(t) + \frac{1}{2}\left[\frac{F(t) + F(t + \delta t)}{m}\right]\delta t \qquad (7)$$

The advantage of this method is that the calculation of velocities is in phase with that of the positions. Also, this method calculates the velocities more accurately than the Verlet and Leap-Frog methods.

The time step δt which is used is about 5 femto second (1femtosecond=1fs=$10^{-15} sec$). The advantage of this algorithm is that the calculation of velocities is in phase with the positions. The initial condition for each molecule is usually assigned by using the Gaussian distribution based on the specified temperature using the following formula:

$$\frac{1}{N_{atm}}\sum_{i=1}^{N_{atm}}\frac{1}{2}m\left|v_i^2\right| = \frac{3}{2}k_B T \qquad (8)$$

The system reaches equilibrium state after 500000 time steps and then NEMD simulations are applied. In all simulation cases, more than 2,000,000 time steps were used for sampling data.

In all simulations, the solid walls are maintained at a specified temperature (saturated temperature for the upper wall and superheated temperature is used for the bottom wall) by coupling them to a Berendsen thermostat [15]. For velocity rescaling, the velocity is first updated from the force acting on the particles and rescaled at each time step according to:

$$V_{new} = \lambda V_{old} \qquad where \qquad \lambda = \left(\frac{T_{t\arg et}}{T_{global}}\right)^{\frac{1}{2}} \qquad (9)$$

Where $T_{t\arg et}$ is the target temperature and T_{global} is the global temperature of the fluid particles in the system. Because the total kinetic energy of a system fluctuates, the instantaneous temperature is defined as a fluctuation of kinetic energy per particle at each slab, per degree of freedom:

$$T_{inst} = \frac{\frac{1}{2}m(V_x^2 + V_y^2 + V_z^2)}{3\,N(Z)\,K_B} \qquad (10)$$

Where $N(z)$ is the number of atoms at height z.

III. BOUNDARY CONDITIONS

Boundaries along the x- and y-directions are periodic, which means that as a particle moves out of the simulation box, an image particle moves in to replace it. But in the z direction, the system is bounded by two solid walls. The thermal wall boundary condition [16] is applied for particles near the walls. In this method, when the liquid particle is near the wall surface, the repulsive force will push the liquid particle away from the wall surface, but some liquid particles may collide with the wall surface. When a particle collides with the bottom wall at the temperature of $T_{sat} + \Delta T$, all three components of the velocities are reset to a biased Maxwellian distribution [16]:

$$v_{xi} = \sqrt{\frac{k_B(T_{sat} + \Delta T)}{m_i}}\psi_1 \qquad (11)$$

$$v_{yi} = \sqrt{\frac{k_B(T_{sat} + \Delta T)}{m_i}}\psi_2 \qquad (12)$$

$$v_{zi} = \pm\sqrt{\frac{-2k_B(T_{sat} + \Delta T)}{m_i}\ln\psi_3} \qquad (13)$$

Where k_B is the Boltzmann constant, m_i is the mass of each molecule, ψ_3 is a uniformly distributed number in range of $(0,1)$, ψ_1 and ψ_2 are Gaussian-distributed random numbers with zero mean and unit variance. Also, when a particle collides with the upper wall at the temperature of T_{sat}, all three components of the velocities are reset to a biased Maxwellian distribution [16]:

$$v_{xi} = \sqrt{\frac{k_B(T_{sat})}{m_i}}\psi_1 \qquad (14)$$

$$v_{yi} = \sqrt{\frac{k_B(T_{sat})}{m_i}}\psi_2 \qquad (15)$$

$$v_{zi} = \pm\sqrt{\frac{-2k_B(T_{sat})}{m_i}\ln\psi_3} \qquad (16)$$

IV. RESULT AND DISCUSSION

Forced annular boiling flow is simulated by imposing an external force, ranging from 1PN to 12PN, to inlet Argon atoms. For all cases after 800000 time steps, the system has evolved into the steady state condition. When the system reaches the steady state, the flow velocity, temperature, surface tension and density profiles are computed as a function of channel height. The program was run for 1500000 time steps for time averaging. In order to compute density, surface tension, liquid film velocity, vapor core velocity and temperature profiles, the domain is divided into $N_{bin,z} = 512$ rectangular bins along the z-direction, each bin with height $\Delta z = \left(L_z/N_{bin,z}\right)$, where L_z is the box length along the z-direction. Also, the domain is divided into $N_{bin,x} = 12$ bins along the x-direction, each bin with length $\Delta x = \left(L_x/N_{bin,x}\right)$, where L_x is the box length along the x-direction. Hence, the volume of each bin is $\Delta x \times \Delta z \times L_y$, where L_y is the box length along the y-direction. For a large number of particles, more bins are needed. For adding molecules in each layer, $H_n(z_i)$ is defined as:

$$H_n(z_{i,j}) = 1 \qquad (n-1)\Delta z \leq z_i \leq n\Delta z$$
$$H_n(z_{i,j}) = 0 \qquad otherwize \qquad (17)$$

Where the subscript j represents the j_{th} time step. Hence, the local average density in the n_{th} slab from time step I_{start} to I_{end} is [17]:

World Academy of Science, Engineering and Technology
International Journal of Physical and Mathematical Sciences
Vol:5, No:6, 2011

$$\rho(z) = \frac{m \sum_{j=I_{start}}^{I_{end}} \sum_{i=1}^{N_{atm}} H_n(z_{i,j})}{L_x L_y \Delta z (I_{start} - I_{end} + 1)} \qquad 0 \le x_i \le \Delta x \qquad (18)$$

Where m is the mass of each molecule and x_i and z_i is the coordinate of the mid-point of the n_{th} slab. When sampling begins, the molecule number in each slab is accounted for and the local density can be considered. Fig.2 shows the effect of the saturation temperature on the density profiles based on the NEMD simulation. It is shown that the liquid molecules in the snapshots are distributed orderly in the neighborhood of the solid interface due to the strong solid liquid interactions. This interface structure and its oscillatory characteristics of the density profiles are in agreement with the majority of earlier works [18,19]. It should be noted that the fluctuating characteristics of the density profiles in this interface structure are due to the fact that the molecules are orderly distributed adjacent to the walls. Also, due to the nanoscale of the distance between the walls, the influence of the wall adsorption on the density of the liquid is very noticeable. In the distance far from the wall, there is an uninterrupted transition for density from the liquid to the vapor zone under different simulation conditions.
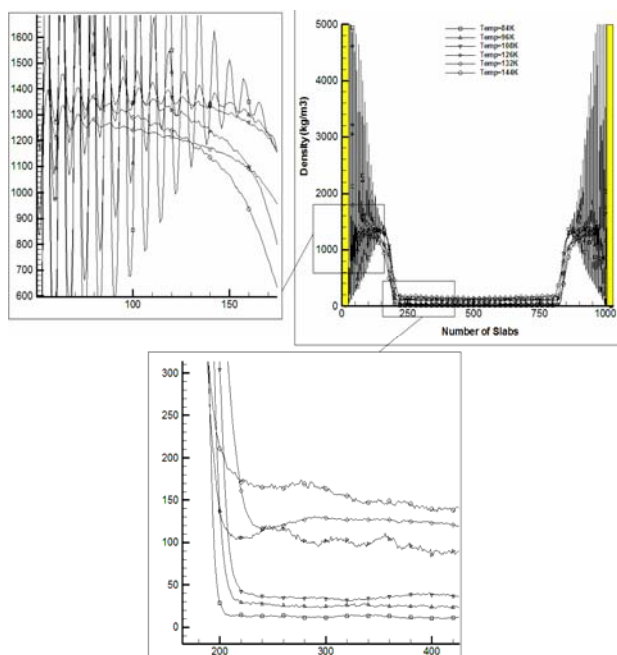
The effect of the magnitude of the external forces on the density profiles is shown in Fig.3.
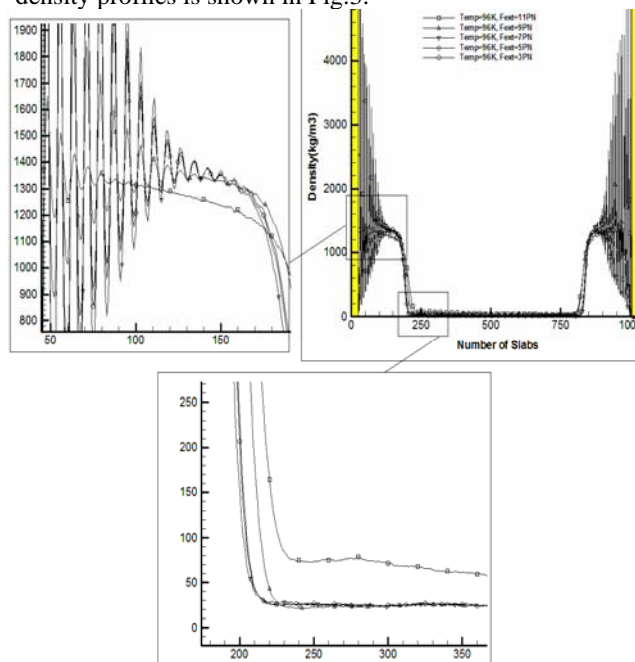
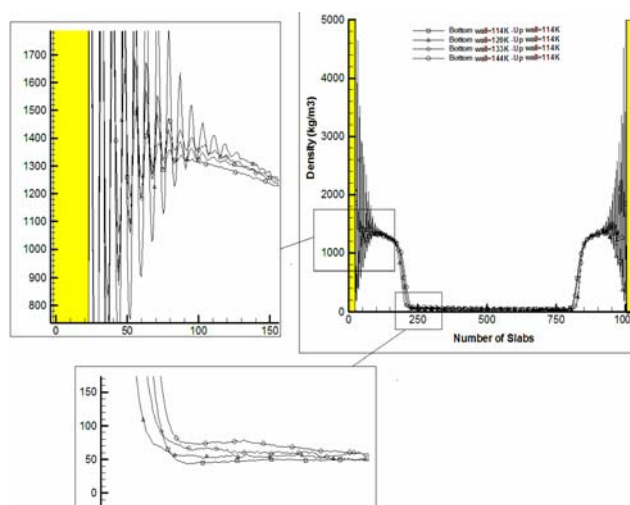Fig. 3 Effect of external force on the density profiles

Fig. 2 Effect of saturation temperature on the density profiles (all particles and solids are at saturation temperature)

Fig.4 Effect of superheated temperature on the density profiles

World Academy of Science, Engineering and Technology
International Journal of Physical and Mathematical Sciences
Vol:5, No:6, 2011

Simulation was carried out at saturation temperature of 84 K with five different external driving forces (per molecule) of 2,4,6,8 and 12 PN at the inlet. It was shown that the driving force had no significant influence on the density profile. This is in agreement with the results reported by Nagayama and Cheng [19]. Therefore, we can conclude that the interfacial density profiles are independent of the magnitude of the driving force.

The effect of superheated temperature on the density profiles is shown in Fig.4 for saturation temperature of 114 K. It is shown that the degree of superheat for the bottom wall has no significant influence on the density profile. Hence, from figures 3and 4 it is concluded that the density profiles are independent of the external driving forces and the degree of superheat for the bottom wall.

At the atomic scale, the surface tension can be expressed as the integrated imbalance of normal and tangential pressure near the interface. The following expressions are used to calculate the two components of the pressure tensor [15],

$$P_N(z) = n(z)k_BT - \frac{1}{2A}\left\langle \sum_{i \neq j} \frac{z_{ij}\phi'(r_{ij})}{r_{ij}} \theta\left(\frac{z-z_i}{z_{ij}}\right)\theta\left(\frac{z_j-z}{z_{ij}}\right)\right\rangle \quad (19)$$

$$P_T(z) = n(z)k_BT - \frac{1}{4A}\left\langle \sum_{i \neq j} \frac{[x_{ij}^2 + y_{ij}^2]\phi'(r_{ij})}{r_{ij}z_{ij}} \theta\left(\frac{z-z_i}{z_{ij}}\right)\theta\left(\frac{z_j-z}{z_{ij}}\right)\right\rangle \quad (20)$$

$$\theta(x) = 1 \quad x \geq 0$$
$$\theta(x) = 0 \quad x < 0 \quad (21)$$

Where the $n(z)$ is the value of density at the height z, the $i<j$ notation indicates a summation over all distinct pairs i and j without counting any pair twice (i.e. as ij and ji), k_B is the Bolzmann's constant, $\langle \ \rangle$ denotes an ensemble average taken over the duration of the simulation for which thermal equilibrium exists. In terms of atomic position and liquid-vapor potential ϕ the expression for surface tension is [15],

$$\gamma_{lv} = \int_{-\infty}^{+\infty}[P_N(z) - P_T(z)]dz \quad (22)$$

Fig.5 shows the local surface tension profile in the direction normal to the interface at saturation temperature of 96 K for different values of driving external forces. In this figure, there are two peaks in each surface tension curve because of the existence of two interfacial zones in the simulation cell. All the surface tension curves fluctuate strongly in traversing the liquid–vapor interface zone, reaching its maximum in the center of the interface zone and spreading fairly in the vapor zones. This figure shows that the driving external force at the inlet of nanochannel has no significant influence on the local surface tension profiles.
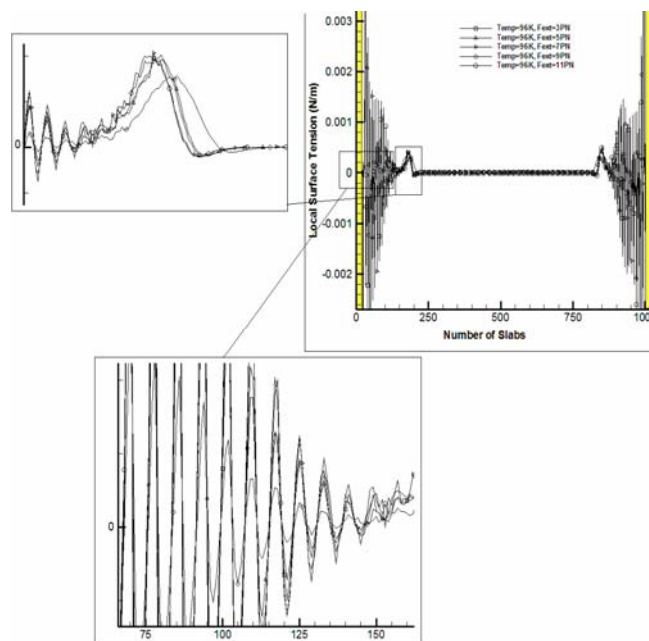

Fig. 5 Local surface tension at different external forces at saturation temperature of 96 K

In this simulation, the local temperature profiles of the simulation domain were calculated from equation 12. These temperature distributions are obtained from the five superheat degrees for the bottom wall and are plotted in Fig.6. From this figure, it is concluded that due to the existence of the superheat degree at the bottom wall, the temperature profiles of the liquid Argon exceed the saturation temperature. Also, the temperature profiles appear to shift up and become discontinuous across the wall- fluid interface. This behavior indicates the presence of a thermal slip (temperature jump) across the wall- fluid interface. In other words, since the local temperature of a system is defined through the thermal velocities of atoms, momentum transfer between the wall and fluid is important. These motions of atoms are influenced by the neighboring atoms of fluid rather than neighboring wall atoms. This causes sudden changes in kinetic energy distribution and causes a temperature jump at the solid-fluid interface. Therefore, heat is generated by the interfacial friction between liquid and solid molecules. Thus, the local temperature near the solid-liquid interface increases and temperature jump occurs at this interface.

World Academy of Science, Engineering and Technology
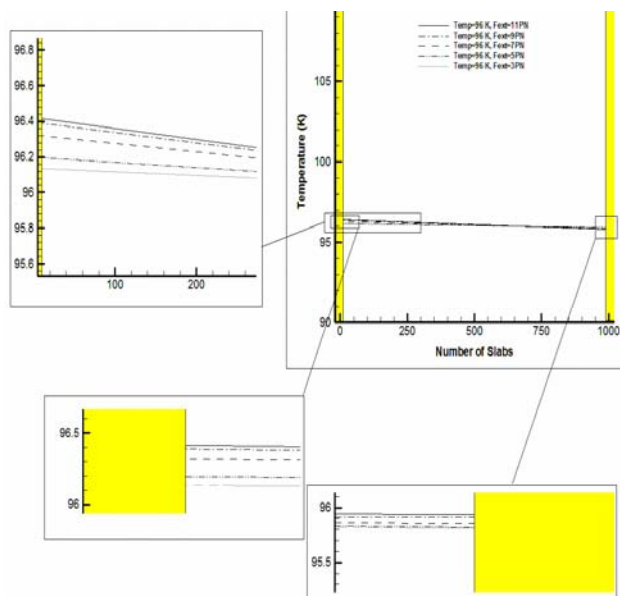International Journal of Physical and Mathematical Sciences
Vol:5, No:6, 2011

Fig. 6 Temperature profiles at different superheated temperature for the bottom wall and at saturation temperature of 96 K for the top wall

The distributions of mean vapor core velocity and mean liquid film velocity along the stream-wise direction are shown in Fig. 7 and 8, respectively. These figures show that due to the relatively strong influence of surface tension in small channel, the interface between the liquid film and vapor core is fairly smooth and the mean vapor core velocity and mean liquid film velocity along the stream-wise direction (x-direction) do not change anymore. This is in good agreement with the majority of earlier works [20] and [7].
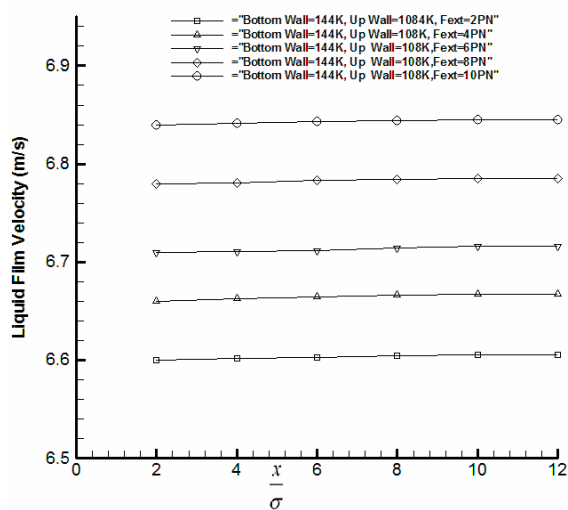

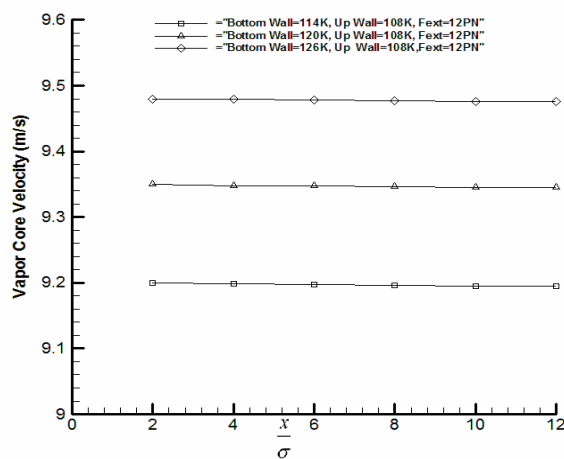Fig. 7 Variation of mean liquid film velocity along the stream-wise direction

Fig. 8 Variation of mean vapor core velocity along the stream-wise direction

V. CONCLUSION

In this paper, the non-equilibrium molecular dynamics simulation of annular boiling flow with *70000* liquid argon atoms in a nanochannel is investigated. The Key findings and conclusions from the present simulation are as follows:

- Surface tension profiles fluctuate in the liquid –vapor interface.
- At higher temperatures and at a higher degree of superheat, the surface tension drops by increasing the temperature.
- The interface between the liquid film and the vapor core is fairly smooth, and the mean velocity along the stream-wise direction does not change anymore.

Further studies aimed to elucidate the precise nature of this flow regime would be of considerable interest. The extension of this paper and our previous works [10, 21, 22] affords engineers a good option for nanochannel simulation in one and two phase flows. Also, future studies aimed at elucidating the precise nature of boiling flow and two phase heat transfer would be of considerable interest.

REFERENCES

[1] D.C. Rapaport, "The art of molecular dynamics simulation", England: Cambridge University Press, 1995.
[2] D. Frenkel, B. Smit, "Understanding molecular simulation – from algorithms to applications", Academic Press, 1996.
[3] L.N. Long, M.M. Micci, B.C. Wong, "Molecular dynamics simulation of droplet evaporation", Comp. Phys. Commun, 1996.
[4] J.R. Lukes, X.G. Liang, and C.L. Tien, " Molecular dynamics study of solid thin-film thermal conductivity" Proceedings of the 1998 International Mechanical Engineering Congress and Exposition November 15-20, Anaheim, California, pp.229-240, 1998.
[5] P. Yi, D. Poulikakos, J. Walther and G. Yadigaroglu, "Molecular dynamics simulation of vaporization of an ultra-thin liquid Argon layer on a surface", International Heat and Mass Transfer, Vol. 45, pp. 2087-2100, 2002.
[6] Z.J. Wang, M. Chen and Z.Y. Guo, "A non-equilibrium molecular dynamics simulation of evaporation", International Conference Passive and Low Energy Cooling for the Built Environment, Santorini, Greece Vol.1, pp. 543-547, 2005.
[7] T. Dong, Z. Yang, H. Wu, "Molecular simulations of R141b boiling flow in micro/nano channel: Interfacial phenomena", Energy Conversion and Management, Vol. 47, pp.2178–2191, 2006.
[8] C.Y. Ji, Y.Y. Yan, "A molecular dynamics simulation of liquid–vapor-solid system near triple phase contact line of flow boiling in a microchannel", Applied thermal engineering, Vol.28, pp.195- 202, 2008.

[9] S.D. Stoddard, P.J. Ford, "Numerical experiments on the stochastic behavior of a Lennard-Jones gas system", Phys Rev A, Vol.8, pp.1504–1512, 1973.

[10] D. Toghraie Semiromi, A.R. Azimian, "Molecular dynamics simulation of liquid–vapor phase equilibrium by using the modified Lennard-Jones potential function", Heat Mass Transfer, Vol. 46, pp.287–294, 2010.

[11] P.A., Thompson, M.O. Robbins, "Shear flow near solids: Epitaxial order and flow boundary conditions", Phys. Rev. A, Vol. 41, pp.6830-6837, 1990.

[12] P. Yi, D. Poulikakos, J. Walther, G. Yadigaroglu, "Molecular dynamics simulation of vaporization of an ultra-thin liquid Argon layer on a surface, Int J Heat Mass Transfer, Vol.45, pp.2087–2100, 2002.

[13] C.Y. Ji, T. Tsuruta, G. Nagayama, "Effects of solid heating surface on nanometer sized liquid films", Thermal Science and Engineering, Vol. 13, pp.25-28, 2005.

[14] G. Sutmann, "Classical molecular dynamics", John Von Neumann Institute for Computing. J ulich, NIC Series, Vol.10, pp.211-254, 2002

[15] J.M. Haile, "Molecular dynamics simulation, elementary methods", Wiley-Interscience Publication, 1997.

[16] F.J. Alexander, A.L. Garcia, "The direct simulation of Monte-Carlo method", Computer Simulation Journal, Vol. 11, pp.588–593, 1997.

[17] J.L. Xu, F.J. Zhou, A.L. Garcia, " Molecular dynamics simulation of micro- Poiseuille flow for liquid argon in nanoscale", J. Heat and Mass Transfer, Vol. 47, pp. 501-513, 2004.

[18] I. Bitsanis, J.J. Magda, M. Tirrell, H.T. Davis, "Molecular dynamics of flow in microscopes", J Chem Phys, Vol.87, pp.173–175, 1987.

[19] G. Nagayama, P. Cheng, "Effects of interface wettability on microscale flow by molecular dynamics simulation", Int. J. of Heat and Mass Transfer, Vol. 47, pp. 501-513, 2004.

[20] S. Somers, H.T. Davis, "Microscopic dynamics of fluids confined between smooth and atomically structured solid surface", J Chem Phys, Vol.96, pp.5389–5407, 1992.

[21] D. Toghraie Semiromi D, A.R. Azimian, "Nanoscale Poiseuille flow and effects of modified Lennard–Jones potential function", Heat Mass Transfer, Vol. 46, pp.791–801, 2010.

[22] D. Toghraie Semiromi D, A.R. Azimian, "Molecular dynamics simulation of nonodroplets with the modified Lennard-Jones potential function", Heat Mass Transfer, Article in press, 2010.